Chapter 3
Behaviour Analysis and Comparison of Tribological Characteristics of Electroless Ni–B Coating under Dry and Lubricated Condition

Santanu Duari, Arkadeb Mukhopadhyay, Tapan Kumar Barman and Prasanta Sahoo

3.1 Introduction

A successful design of machine element depends on the understanding of tribological principles. The word 'tribology' has been derived from Greek word 'tribos' which means rubbing. Tribology may be defined as the science and technology of contacting surfaces under relative motion. Tribological behaviour depends on rubbing surface of material with or without the effect of environment. Due to advancements in technology, nowadays various methods have been developed for surface modification [1]. In tribology, friction and wear are necessary evils which cannot be eliminated but needs to be controlled or minimized for the effective working of a machine element as well as improved working life. Thus, the study of tribology is an important and essential part. It applies operational analysis for attributes of great economic importance such as reliability, maintainability and wear of technical equipment ranging from a simple household appliance to a complex spacecraft.

In the present era, the purpose of deposition of metallic coatings is to serve as a protective layer to the base material against wear and corrosion. Friction and wear are two decaying marvels which are the wellsprings of significant misfortune in mechanical components. They do not just decrease the life of the modern machine components but also result in increase in cost and maintenance. Since friction, corrosion and wear are surface phenomenon, they can be controlled by surface treatment. Electroless deposition is by far a much better way to overcome such type of problems rather than any other coatings. Electroless deposition of metals was first demonstrated in 1844 [2]. However, the first practical system for electroless coating was developed by Brenner and Riddell after a century [3].

S. Duari (✉) · A. Mukhopadhyay · T. K. Barman · P. Sahoo
Department of Mechanical Engineering, Jadavpur University, Kolkata, India
e-mail: santanu_duari@yahoo.co.in

Electroless plating is an autocatalytic procedure where the substrate builds up a potential when it is immersed in an electroless setup called bath that contains a source of metallic ions, complexing agent, reducing agent, buffers, stabilizer, wetting agents and different components. Nickel sulphate and nickel chloride salts are generally used as the source of nickel ion. However, nickel hypophosphite [Ni $(H_2PO_2)_2$] has been considered the ideal source of nickel ion [4–7]. Sodium borohydride ($NaBH_4$) is a strong reducing agent for the electroless nickel (EN) plating process [8–11]. Investigations have been also carried out using hydrazine as a reducing agent for deposition of pure nickel, palladium and gold [12]. But the use of hydrazine has been discontinued since it is very difficult to control and its associated hazards [13]. In order to prevent the decomposition of the solution and to make the bath stable, the complexing agents are added to the electroless bath [14]. Buffering agents are used to control the pH of the bath. Effect of pH on the plating rate of electroless nickel deposits has been also carried out [15]. Stabilizer content even in significantly low amounts may slow down the reaction rate [14]. Surfactants tend to lower the surface tension and hence permit lowering the interfacial tension between two liquids or a liquid and solid surface. Sodium dodecylsulphate (SDS) and cetyltrimethyl ammonium bromide (CTAB) are used as a surfactant for electroless Ni–P coating [16].

A number of advantages of using electroless nickel coating method over other coating method are as follows [5]:

- Resistance against wear and corrosion;
- Increase in microhardness and thermal resistance;
- Smooth and uniform deposit regardless of the geometry of the substrates;
- Good solderability, bondability, weldability, chemical stability and non-magnetic properties;
- Greater lubricity and high thermal conductivity.

The physical and chemical properties of electroless nickel coatings depend upon bath formulation and conditions of operation. The microstructures and properties of EN coatings are dependent on phosphorous content alloyed in the deposit [17–19]. Annealing affects the properties of electroless nickel coatings by changing its microstructure [6, 20, 21]. Electroless Ni–B coatings are found to exhibit an extremely smooth surface [22]. Heat treatments of the coating cause a further degradation of normal and maximal roughness [22, 23].

From the literature, it may be comprehended that several studies have been focused on the investigation of tribological properties of electroless nickel coatings. Electroless nickel–phosphorus is the most popular variant due to its excellent tribological and anti-corrosion characteristics [24–26]. Ni–B coating is comparatively newer and is a hard variant of the EN family. But most of the literatures concerning the tribological characteristics of Ni–B coatings have been carried out under dry sliding condition [27–32]. But it has also been observed that the microstructure of Ni–B coatings is such that they are naturally/inherently self-lubricious. Furthermore, the nodulated structures and columnar growths also have the

capability of retaining lubricants. Therefore, it is necessary to investigate the tribological behaviour of Ni–B coatings under lubrication. The suitability of electroless Ni–B as a tribo-coating under lubricated condition is assessed in the present work. A comparison with the tribological behaviour under dry condition is also carried out. Flow diagram of the present work is shown in Fig. 3.1.

3.2 Materials and Methods

3.2.1 Preparation of Substrate and Coating Deposition

Coating deposition is carried out on cylindrical steel (AISI 1040) substrates of dimension Ø6 × 30 mm. This specific measurement of the specimen is selected in accordance with its counterpart in the tribotesting setup where the sample must be attached for tribological testing. Electroless coatings follow the profile of the substrate on which it is deposited. Hence, wear and frictional force may be dependent on the surface roughness of the coating, which in turn depends on surface roughness of the substrate. In the present work, the centre line average roughness (R_a) of the coatings is 0.4 µm (corresponding to N5 roughness grade). Before coating, the substrates are rinsed in deionized water. Then, acetone is used for degreasing and removal of corrosive or any remaining organic products. Finally, before deposition, the substrates are subjected to pickling treatment in HCl solution for the removal of oxide layers which may have formed. Finally, the samples are rinsed in deionized water and dipped into the electroless bath.

The electroless bath is prepared by mixing the chemicals as shown in Table 3.1. The chemicals are measured on an electronic balance of high precision. Two beakers with 250 ml volume are properly cleaned and then rinsed using deionized water for preparation of the electroless bath. In one of the beakers (A), 100 ml deionized water is taken and the same volume of water is taken in another beaker (B). In beaker A, the chemicals (nickel chloride, ethylenediamine, sodium hydroxide and lead nitrate) are taken in proper quantity along with sequence given and mixed on a magnetic heater cum stirrer. In beaker B, the chemicals (sodium hydroxide and sodium borohydride) are taken sequentially and mixed by stirrer. The solutions in the two beakers are mixed to form a total bath volume of 200 ml. The pH of the solution is measured to be around 12.5 using pH strips and it was maintained constant throughout the deposition process. Upon heating the solution, the substrate initiates the autocatalytic chemical reduction process. The samples are dipped into the chemical bath keeping temperature constant at 90 ± 2 °C for deposition time of about 2 h. It is ensured that a uniform value of coating thickness is maintained in all samples by controlling chemical bath composition and deposition condition. The coated specimen is taken out from bath and washed with deionized water. The schematic diagram of the electroless coating deposition setup is presented in Fig. 3.2.
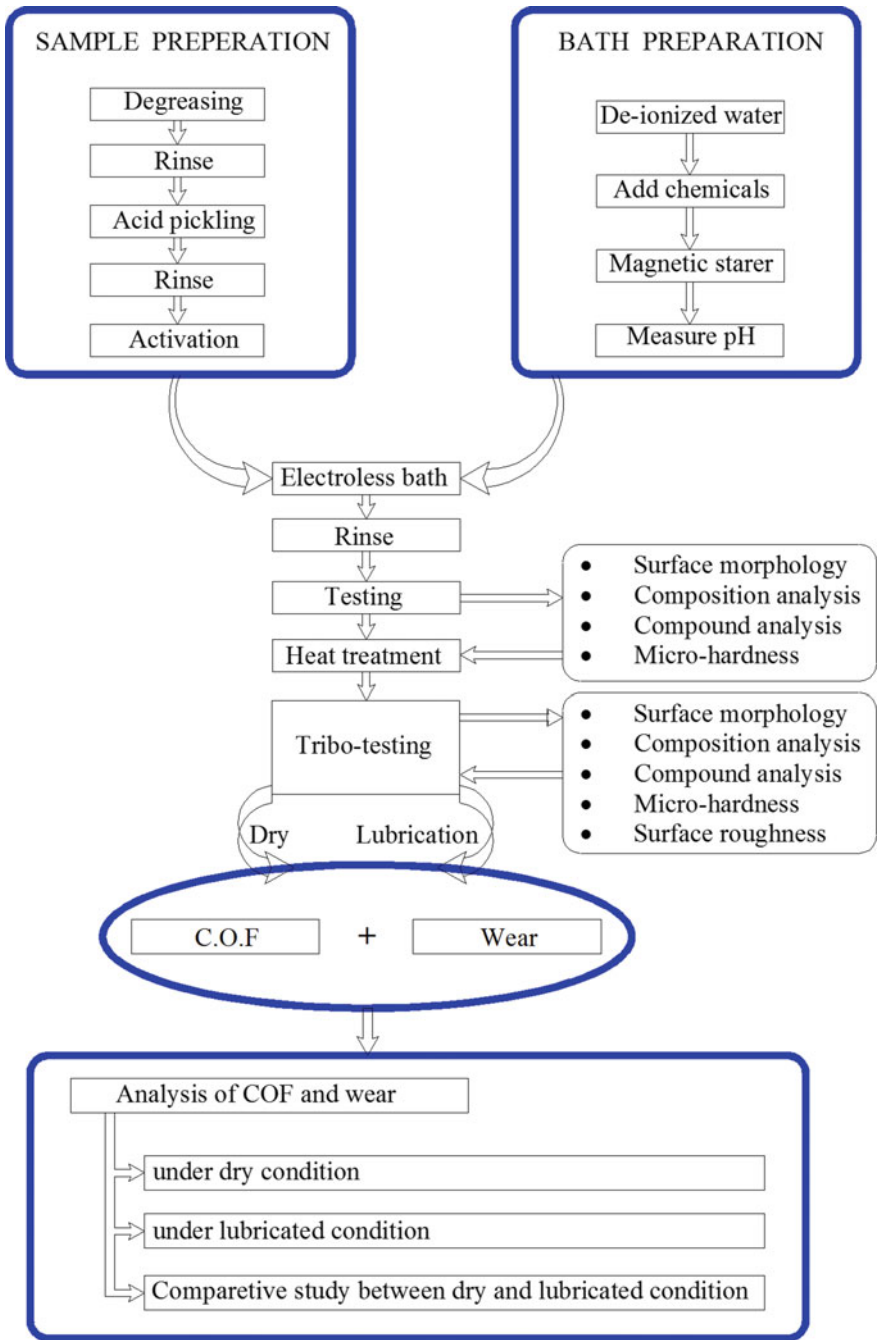
SAMPLE PREPERATION

Degreasing

Rinse

Acid pickling

Rinse

Activation

BATH PREPARATION

De-ionized water

Add chemicals

Magnetic starer

Measure pH

Electroless bath

Rinse

Testing

- Surface morphology
- Composition analysis
- Compound analysis
- Micro-hardness

Heat treatment

Tribo-testing

- Surface morphology
- Composition analysis
- Compound analysis
- Micro-hardness
- Surface roughness

Dry   Lubrication

C.O.F   +   Wear

Analysis of COF and wear

under dry condition

under lubricated condition

Comparetive study between dry and lubricated condition

Fig. 3.1 Flow diagram of experiment and analysis

Table 3.1 Composition and deposition condition of chemical bath

Bath constituents	Role of chemicals	Values	Unit
Nickel chloride	Source of nickel ion	20	g/l
Sodium borohydride	Reducing agent	0.8	g/l
Ethylenediamine	Complexing agent	59	g/l
Lead nitrate	Stabilizer	0.0145	g/l
Sodium hydroxide	Buffer	40	g/l
Bath temperature		90 ± 2	°C
pH of solution		12.5	
Deposition time		2	hr
Bath volume		200	ml
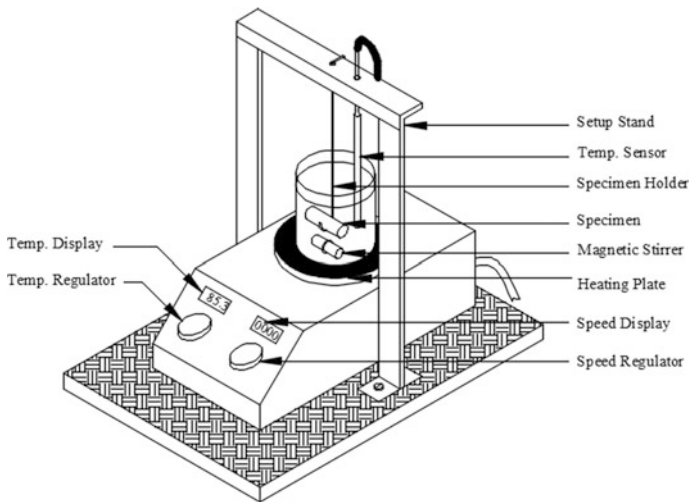
Fig. 3.2 Schematic diagram of the electroless coating deposition setup

The coated specimens are annealed in a muffle furnace with a size of $100 \times 100 \times 220$ mm^3. Annealing temperature is kept constant to maintain almost same hardness of all the specimens. Heat treatment is done at 350 °C for one hour. After heating, the samples are held inside the chamber and allowed to cool down to ambient temperature without the application of any artificial cooling.

3.2.2 Coating Characterization

The composition of EN depositions significantly determines the phase structure and tribological behaviour. Heat treatment results in an improved hardness,

wear resistance and low friction coefficient. Due to this, it is important to study the coating characteristics in detail and to understand their effect on wear behaviour. The surface morphology, bath composition and phase transformation characteristics of the coatings have been examined by scanning electron microscope (SEM), energy dispersive X-ray analysis (EDX) and X-ray diffraction analysis (XRD), respectively. SEM and EDX analysis are done on a FEI Quanta 250 equipment, whereas XRD is carried out on a Rigaku Ultima III equipment.

3.2.3 Hardness Study of the Coating

Hardness is defined as the reluctance of a material to permanently deform, or indent. Hardness indicates the ability of a material to resist permanent deformation by another harder material and its resistance to plastic deformation. There are several hardness testing mechanisms such as scratch hardness, indentation hardness and rebound hardness. The hardness of a material depends on the ductility, elastic stiffness, plasticity, strain, strength and toughness of the material. Scratch hardness denotes the resistance of a material to fracture or plastic deformation due to friction from a sharp object. Various indentation hardness tests include Vickers hardness test, Knoop hardness test, Brinell's hardness test, Rockwell's hardness test, etc.

Here, Vickers hardness test is carried out to measure the microhardness of thin coatings with the help of UHL microhardness apparatus (VMHT MOT, Technische Mikroskopie) with a Vickers diamond indenter (Fig. 3.3a). It is generally based on the indentation formed by a diamond indenter onto the material. The basic principle of Vickers hardness test is to observe the ability of the material under question to resist plastic deformation. Vickers hardness (HV) is calculated according to the following formula:

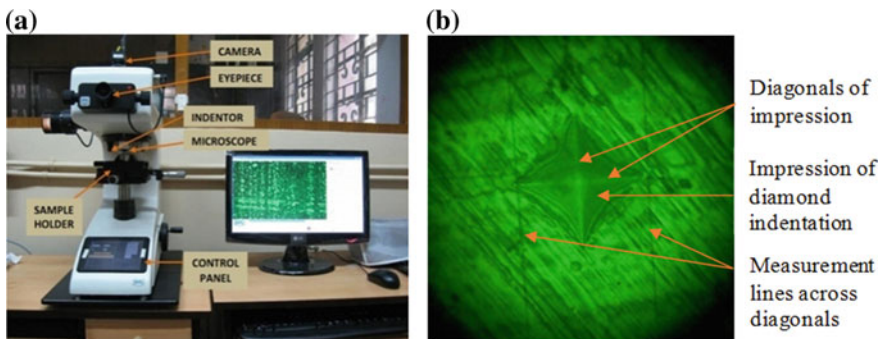$$HV = 0.1891 \frac{F}{d^2} \qquad (3.1)$$

Fig. 3.3 a Photograph of microhardness testing machine **b** Microscopic image of impression

where F is the load in kilogram-force and d is the average length of the two diagonals (shown in Fig. 3.3b) created by the pyramidal diamond indenter onto the surface of the material in millimetres. The indentation is done with Vickers diamond indenter with load of 500 g, dwell time of 15 s and approach velocity of 25 μm/s. A mean of at least six hardness data for each sample is taken.

3.2.4 Roughness Study of the Coating

Surface roughness describes the morphological features of a surface. Any surface is not plane or smooth as it appears but covered with microscopic hills, valleys and even scratches. Surface roughness is a bulk measure of the average size of the hills and valleys. Surface roughness is critical to the performance of wear-resistant and self-lubricating coatings, stress corrosion and fatigue. Wear and friction are influenced by surface roughness and in many instances; an optimum roughness can be found which provides a minimum of wear and friction. For coatings proposed to present high corrosion resistance, excessive roughness can be an indication of low-quality coatings.

Centre line average or R_a is the arithmetic mean value of the departure of the profile from the centre line along the length given below:

$$R_a = \frac{1}{L}\int_0^L |Z(x)|\,\mathrm{d}x \tag{3.2}$$

where $Z(x)$ is the height of the surface above mean line at a distance x from the origin and L is the measured length of the profile as shown in Fig. 3.4. The surface roughness parameter R_a on the coated surfaces is estimated with the Talysurf (Surtronic 3+, Make—Taylor Hobson, UK). It is equipped with a diamond stylus with a tip radius of 5 μm.
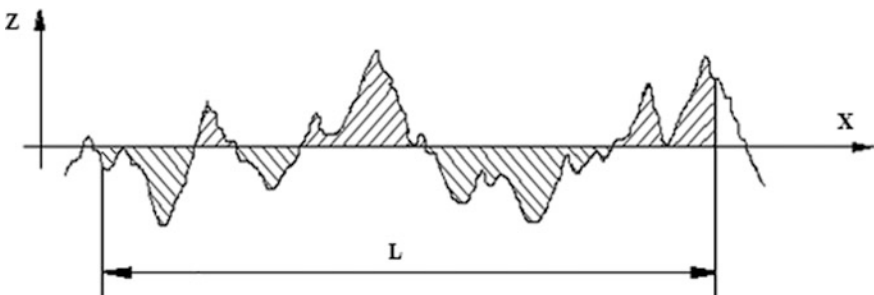

Fig. 3.4 Center line average of a surface over the sampling length L

In this study, the measurements are taken at 0.8 mm sampling length and 4 mm traverse length. Roughness measurements on the coated samples have been repeated six times. The measured profile of Talysurf is digitized by the advanced surface finish analysis software Talyprofile for evaluation of the roughness parameter R_a.

3.2.5 Tribological Tests

The friction and wear tests of EN coatings are carried out on a pin-on-disc type setup with a data acquisition system (TR-20LE-CHM-400, Ducom, India). The applied normal load, rotational speed of counterface disc and sliding duration are varied. The track diameter is set at 80 mm. A photograph of the tribotester is shown in Fig. 3.5. The coated specimens press against a rotating counterface disc of dimensions Ø165 × 8 mm (material: hardened EN31 steel). The speed and time for which the disc rotates can be controlled using the controller device provided with the tribotester. The normal load is applied by placing dead weights on a loading pan attached to a loading lever that transmits the normal load to the specimen at a ratio of 1:1. A load cell measures the frictional force. A linear variable differential transformer (LVDT) measures the wear depth (µm) of the specimens. Friction and wear tests are conducted under both dry and lubricated condition. For dry condition, testing is done under normal ambient condition without providing any lubricant. For the sliding wear tests under lubricated condition, Servo PRIDE 40,
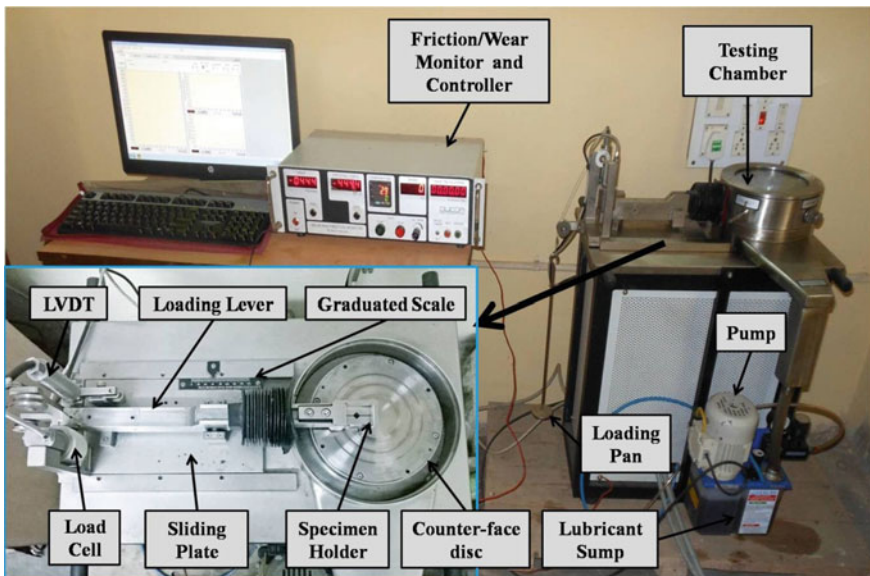

Fig. 3.5 Pin-on-disc type tribotester (TR-20LE-CHM-400)

Table 3.2 Characteristics of lubricant used

SAE Grade	PRIDE 40
Kinematic viscosity, cSt @ 100 °C	13–15
Viscosity index, Min.	90
Flash point (Cleveland open-cup method), °C Min.	220
Pour point, °C Max.	(−) 6
Total base number (TBN) mg KOH/gm	9.5–12.5

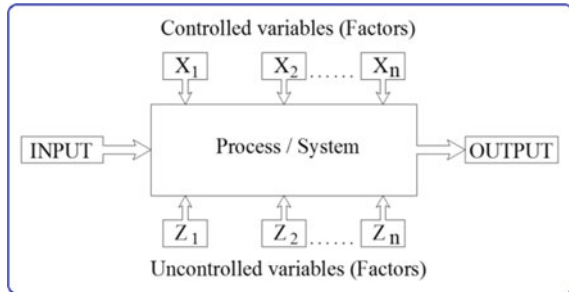**Fig. 3.6** General model of a particular process or system

Table 3.3 Test parameters along with their levels for behaviour analysis

Design factors	Unit	Levels				
		1	2	3	4	5
Load (L)	N	10	15	20	25	30
Speed (S)	RPM	60	70	80	90	100
Time (T)	Min.	3	6	9	12	15

manufactured by Indian Oil, is used which is an engine oil. The properties of the lubricating oil are shown in Table 3.2.

Experiments are carried out following full factorial design [33, 34]; that is, it includes all and every individual combination of levels and parameters. A general model of experimental design technique for investigation of a system is shown in Fig. 3.6. Here, three most important parameters, viz. applied load, rotating speed of counterface disc and duration of sliding, have been selected as tribological testing parameters. Their values at different levels are laid down in Table 3.3. The design parameters have been divided into equally spaced levels.

3.3 Results and Discussion

Electroless Ni–B is deposited on AISI 1040 specimen. Coating characterization is done using SEM, EDX and XRD to ensure and analyse the uniformity of the deposits. The microhardness and surface roughness of electroless Ni–B deposits are

also reported. Variations of friction and wear with process parameters are described for dry and lubricated conditions. An attempt has been also made to compare the coefficient of friction (COF) and wear depth under dry and lubricated sliding condition.

3.3.1 Coating Characterization

3.3.1.1 Surface Morphology

SEM micrographs of electroless Ni–B in as-deposited condition and post-annealing (350 °C for 1 h) condition have been presented in Fig. 3.7. The coated surface seems to have a cauliflower-like appearance which makes it self-lubricating in nature. Also, no surface damage can be observed. The surface appears to be grey in colour. Compared to the as-deposited SEM micrograph, the heat-treated deposit is more inflated. The nodules of the coating increase in size with heat treatment, whereas in as-deposited condition they are more flat and deflated.

A cross section of the deposit has been shown in Fig. 3.8 that reveals uniform deposit thickness and columnar structures. The coating thickness is ∼30 μm and seems to be well connected to the substrate.

3.3.1.2 Analysis of Composition

To ensure the deposition of nickel and boron on the mild steel substrate, EDX is used. The EDX spectrum of the coated samples in as-deposited condition is displayed in Fig. 3.9. The peaks of nickel and boron are quite specific. Boron content is seen to be around 7.51% by weight while the remaining is mostly nickel.
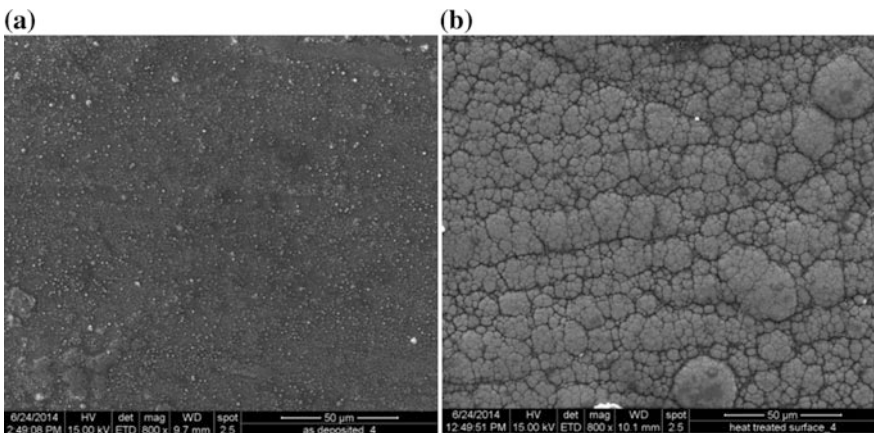

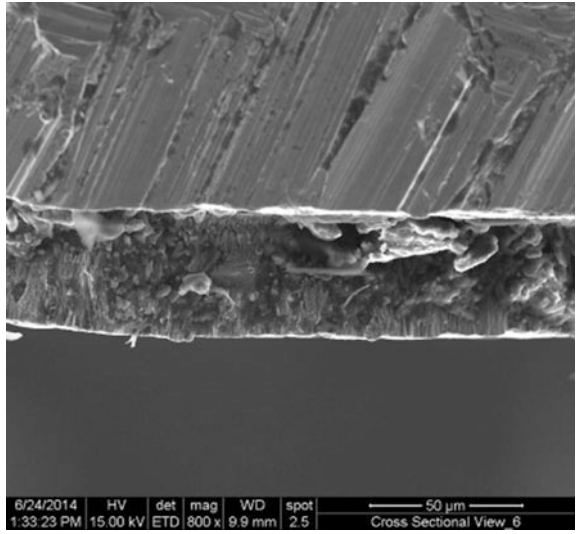**Fig. 3.7** SEM micrograph of Ni–B coating **a** as-deposited **b** annealed at 350 °C

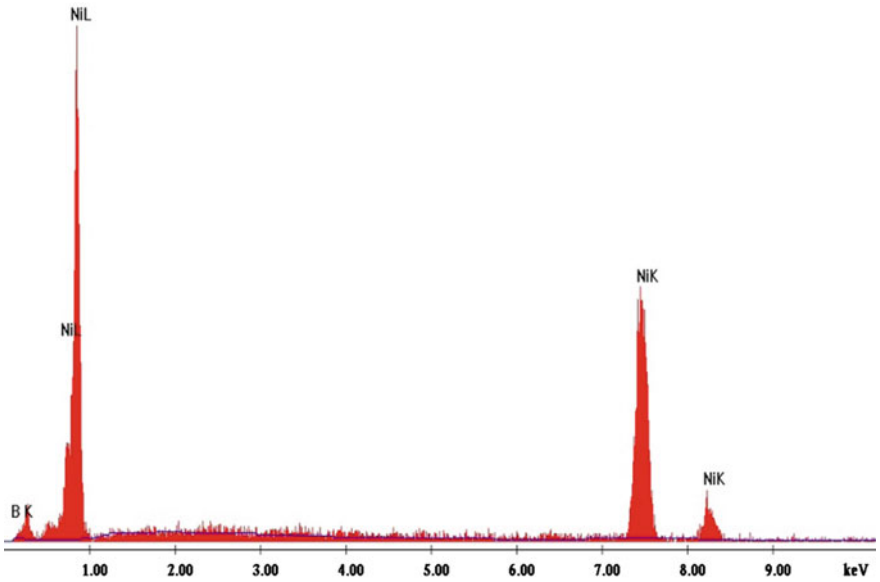**Fig. 3.8** SEM micrograph of cross cut of as-deposited Ni–B coating

Fig. 3.9 EDX spectrum of Ni–B coating

3.3.1.3 Analysis of Phase Transformation

The XRD plots for as-deposited as well as heat-treated deposits are shown in Fig. 3.10a, b, respectively. It is observed from the plots that in as-plated condition, electroless Ni–B coating exhibits a single broad peak which indicates that it is amorphous in nature. Transformation of amorphous state to crystalline takes place due to heat treatment. The XRD pattern of electroless Ni–B coating post-annealing confirms the formation of Ni_3B and Ni_2B crystalline phases.

3.3.1.4 Microhardness Study

The microhardness values of the deposits have been measured in as-deposited and heat-treated condition to mark the effect of heat treatment on electroless Ni–B coating. The average values of hardness in as-deposited and heat-treated condition are seen to be 855 $HV_{0.5}$ and 1160 $HV_{0.5,}$ respectively. Thus, there is a significant rise in the value of hardness. The values of hardness for all the 125 samples are presented in Fig. 3.11. The formation of hard nickel borides results in the increased hardness of electroless Ni–B coatings in heat-treated condition resulting from precipitation hardening phenomenon. Nickel borides may be impeding the movement of dislocations (defects in crystal lattice) and in this manner contributes to the strength of the deposition.

3.3.1.5 Roughness Study

Surface roughness plays an important role in controlling friction and wear. Before subjecting the Ni–B coatings to tribological tests, surface roughness of all the samples is measured. To ensure that results of tribological tests are not affected by
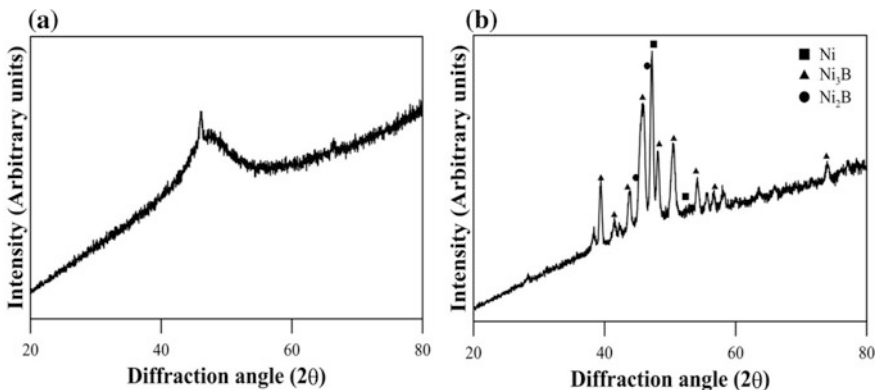

Fig. 3.10 XRD pattern of Ni–B coating **a** as deposited and **b** heat treated at 350 °C
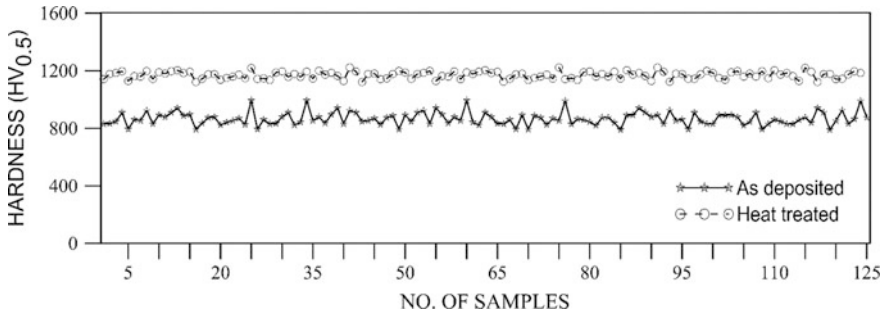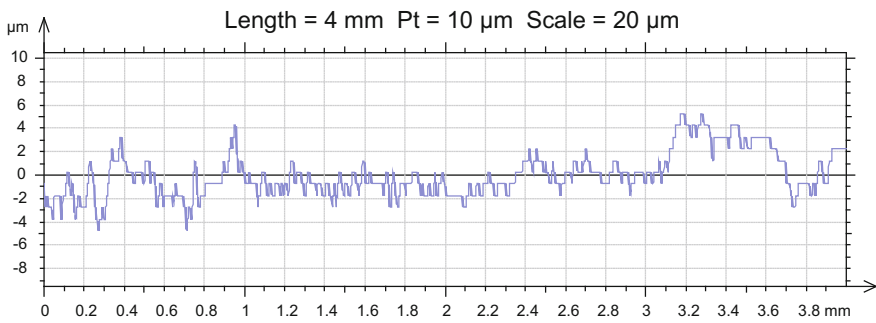
Fig. 3.11 Microhardness of Ni–B coating

Fig. 3.12 Surface roughness of Ni–B coating

the surface roughness, the coatings having R_a value $\sim$0.7–0.8 µm are selected for the experimental runs. Surface profile of one of the samples is shown in Fig. 3.12.

3.3.2 Friction and Wear Behaviour

Experiments for investigation of friction and wear are conducted on a pin-on-disc type tribotester as shown in Fig. 3.5 following the full factorial design. Tests are completed in two different environments, i.e. dry and lubricated condition. Properties of the lubricant are also presented in Table 3.2. Data for friction and wear depth are collected from the tribotester for all possible combination of design parameters, i.e. applied load, speed and sliding duration. Variation of friction and wear with process parameters under dry and lubricated conditions are studied.

3.3.2.1 Friction and Wear Behaviour Under Dry Condition

Figure 3.13a, b represents the variation of COF versus sliding duration at various sliding speeds when the load is kept constant at 10 and 30 N, respectively. It is noticed that with the increase of sliding speed, COF increases. So it can be concluded that COF varies inversely with load and directly with speed. Figure 3.14a, b shows the variations of COF versus sliding time with varying applied normal loads and at constant sliding speeds of 60 and 100 rpm, respectively. It is found that for any constant sliding speed, friction coefficient gradually increases with sliding duration. The COF decreases with an increment in applied load at 60 rpm as well as 100 rpm. But the COF seems to be quite low and comparable with that reported by other researchers for EN coatings [21, 23]. The low COF of electroless Ni–B coating can be mainly attributed to its microstructure and self-lubricating property. The rise in frictional force is not significant enough to cause an increase in the value of COF of the deposits.
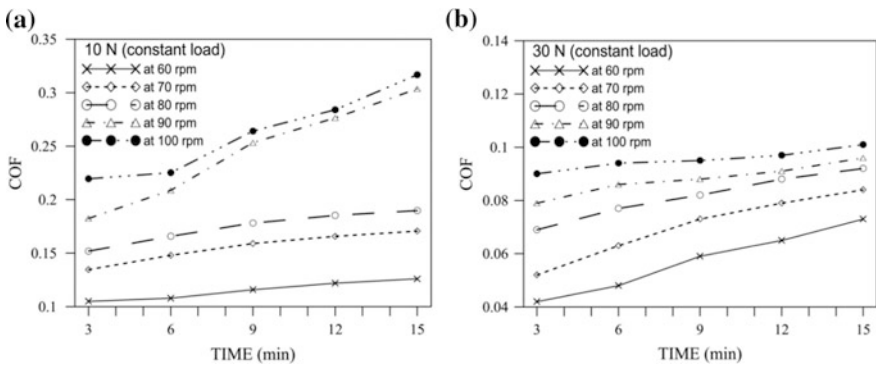

Fig. 3.13 COF versus sliding duration of Ni–B coating with different sliding speed at constant load of **a** 10 N and **b** 30 N under dry condition
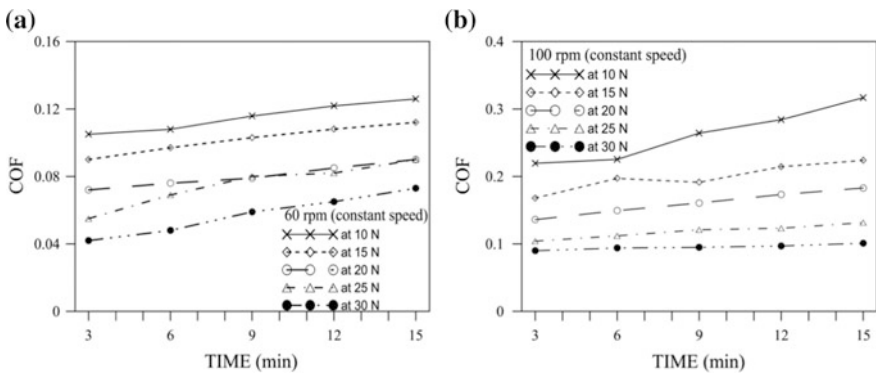

Fig. 3.14 COF versus sliding duration of Ni–B coating with different load at constant speed of **a** 60 rpm and **b** 100 rpm under dry condition

Figure 3.15a, b shows the variation of wear depth with sliding duration at various speeds keeping the load constant at 10 and 30 N, respectively. In Fig. 3.15a, b, wear depth increases with speed at 10 and 30 N, respectively. In fact, the wear depth also increases significantly with duration of sliding. But the increase in wear depth with sliding speed is gradual and not drastic within 60–100 rpm at 10 N as well as 30 N.

Figure 3.16 shows the variation of wear depth with sliding time at constant speed and at different normal loads. Figure 3.16a represents the variation of wear depth at a constant speed of 60 rpm (at the lowest sliding speed). From this plot, the following observations may be made: (i) with sliding time, wear depth increases and (ii) as the normal load increases, the wear depth increases. Figure 3.16b represents the same trend at a sliding speed of 100 rpm (at the highest sliding speed). From these two graphs, it is also seen that in general at higher speed the wear depth
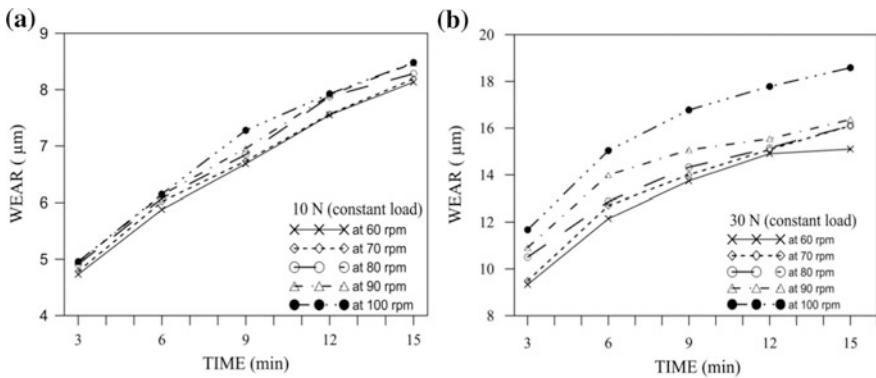

Fig. 3.15 Wear versus sliding duration of Ni–B coating with different sliding speed at constant load of **a** 10 N and **b** 30 N under dry condition
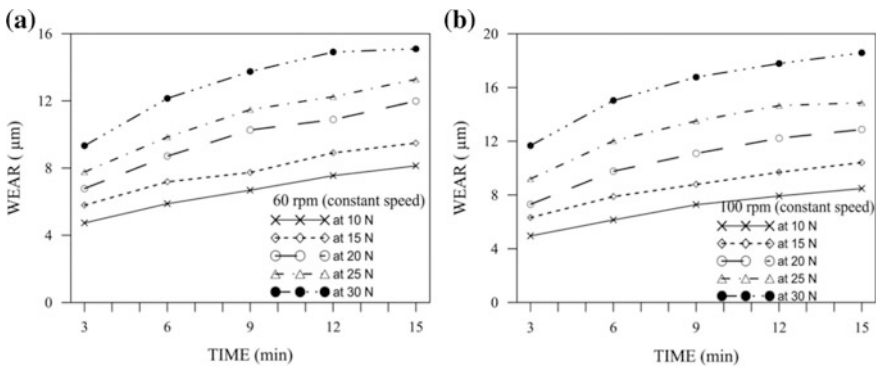

Fig. 3.16 Wear versus sliding duration of Ni–B coating with different load at constant speed of **a** 60 rpm and **b** 100 rpm under dry condition

is higher. In fact at 100 rpm (Fig. 3.16b), the increase in wear depth is quite high. Compared to 10 N load, wear depth increases by almost three times when the load is increased to 30 N. Finally, it is concluded that wear depth increases with applied load as well as sliding speed.

When normal load increases, the interacting surfaces advance more towards each other. A greater number of asperities come in contact and also the contact radius of the individual asperities increases which leads to an increase in contact area of the asperities. This results in an increase in the volume of material that is being shared by the rotating counterface material of the tribotester. Hence, the wear depth increases. So the minimum wear may be found at low levels of load, speed and sliding time.

3.3.2.2 Friction and Wear Behaviour Under Lubricated Condition

In this section, COF and wear characteristics are studied under lubricated condition. Figure 3.17 represents the effect of normal load on COF at different sliding speed with respect to duration of sliding. At 10 N as well as 30 N, the COF is almost constant with an increase in sliding duration. At 10 N, the COF initially decreases with speed and then increases. But at 30 N, the variation of COF at 70–100 rpm is very less and is almost comparable.

The variations of COF are shown in Fig. 3.18a, b with different load and sliding duration at constant speed of 60 and 100 rpm, respectively. It is found that at any constant speed, COF gradually increases with increasing load. The COF for all the cases observed in Figs. 3.17 and 3.18 exhibits an initial abrupt increase, followed by a slow rise during the first few seconds of sliding. The decrease in friction with the increase in load could be due to the self-lubricating nature of the deposition and the ability of the nodules to retain lubricants.
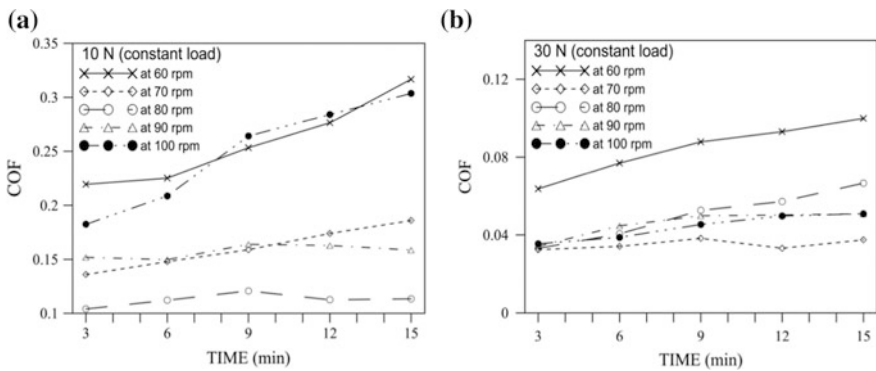

Fig. 3.17 COF versus sliding duration of Ni–B coating with different sliding speed at constant load of **a** 10 N and **b** 30 N under lubricated condition
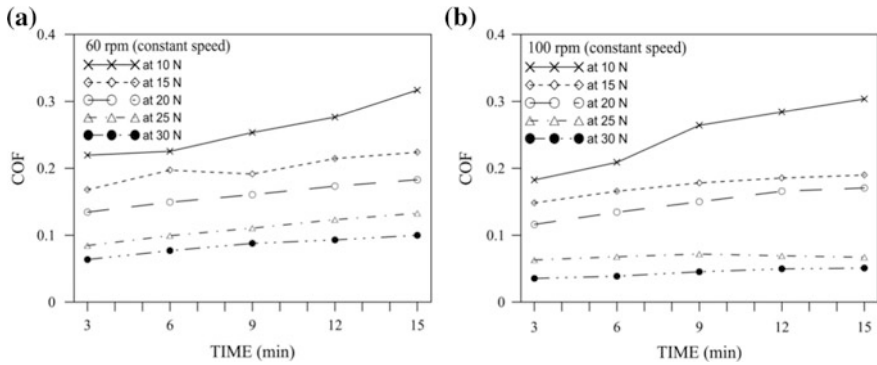
Fig. 3.18 COF versus sliding duration of Ni–B coating with different load at constant speed of **a** 60 rpm and **b** 100 rpm under lubricated condition

Figure 3.19 shows the effect of normal load on wear depth at different sliding speed regarding sliding duration. Figure 3.19a, b represents the variation of the depth of wear with sliding speed and sliding duration at constant load of 10 and 30 N, respectively. It is found that any constant load wear is gradually increasing with increase in rotating speed and sliding duration.

Figure 3.20a, b represents the wear depth with the variations of normal load and sliding time at constant speeds of 60 and 100 rpm, respectively. It is found that at any constant speed, wear gradually increases with load as well as sliding time. At 60 rpm as well as 100 rpm, the wear depth at 30 N is quite higher compared to that observed at 10 N ($\sim$3 times) especially after a sliding duration of 15 min.
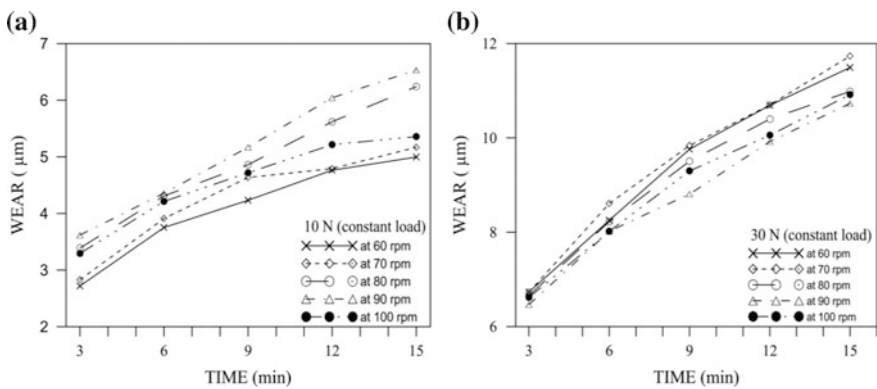

Fig. 3.19 Wear versus sliding duration of Ni–B coating with different sliding speed at constant load of **a** 10 N and **b** 30 N under lubricated condition
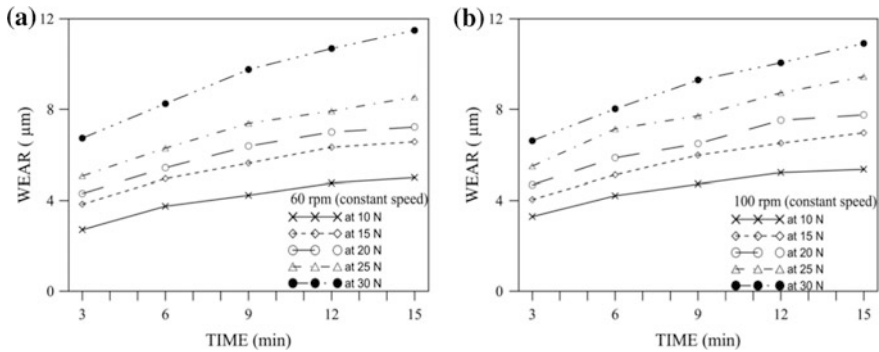
Fig. 3.20 Wear versus sliding duration of Ni–B coating with different load at constant speed of **a** 60 rpm and **b** 100 rpm under lubricated condition

3.3.2.3 Comparison of Friction and Wear Characteristics Under Dry and Lubricated Conditions

Comparative study of tribological characteristics of electroless Ni–B deposition has been carried out by generating 3D surface plots and shown in Figs. 3.21 and 3.22. In each of the 3D surface plots, two design parameters are varied while the third variable is kept fixed at its mid-level value.

The variation of COF under dry and lubricated conditions with load and speed is shown in Fig. 3.21a. It is noticed that COF under lubricated condition is lower at higher values of normal load and sliding speed compared to the dry condition. But at lower loads and speeds, the COF under dry condition is lower compared to lubricated condition. This may be due to inadequate film formation at lower values of applied load and rotating speed. Moreover, at a lower speed, there are chances that debris particles formed may get trapped in the lubricant leading to a higher COF [35]. But at higher speeds, it is expected that adequate lubrication occurs and the film provides lubricating effect. Moreover, at higher speeds, due to the centrifugal action of the counterface disc the debris may get carried away by the flowing lubricant. It has been also observed that tribo-oxidative layers form under lubricated condition [36]. They tend to lower the COF. Thus, under lubricated condition, an improvement in COF takes place especially at higher values applied load and rotating speed. The variation of COF with load and time may be observed in Fig. 3.21b. In this plot, it is seen that with an increase in sliding duration, the COF under lubricated condition improves significantly compared to dry condition. This could be due to the fact that a stable tribo-patch is formed with an increase in time. The variation of COF with sliding speed and duration may be observed in Fig. 3.21c. A curvature in the plot may be seen and the COF is quite lower under lubricated condition compared to dry condition especially at higher values of speed.

The wear depth of the deposits under dry and lubricated condition with different load and sliding speed is shown in Fig. 3.22a. In fact, the trends observed for the
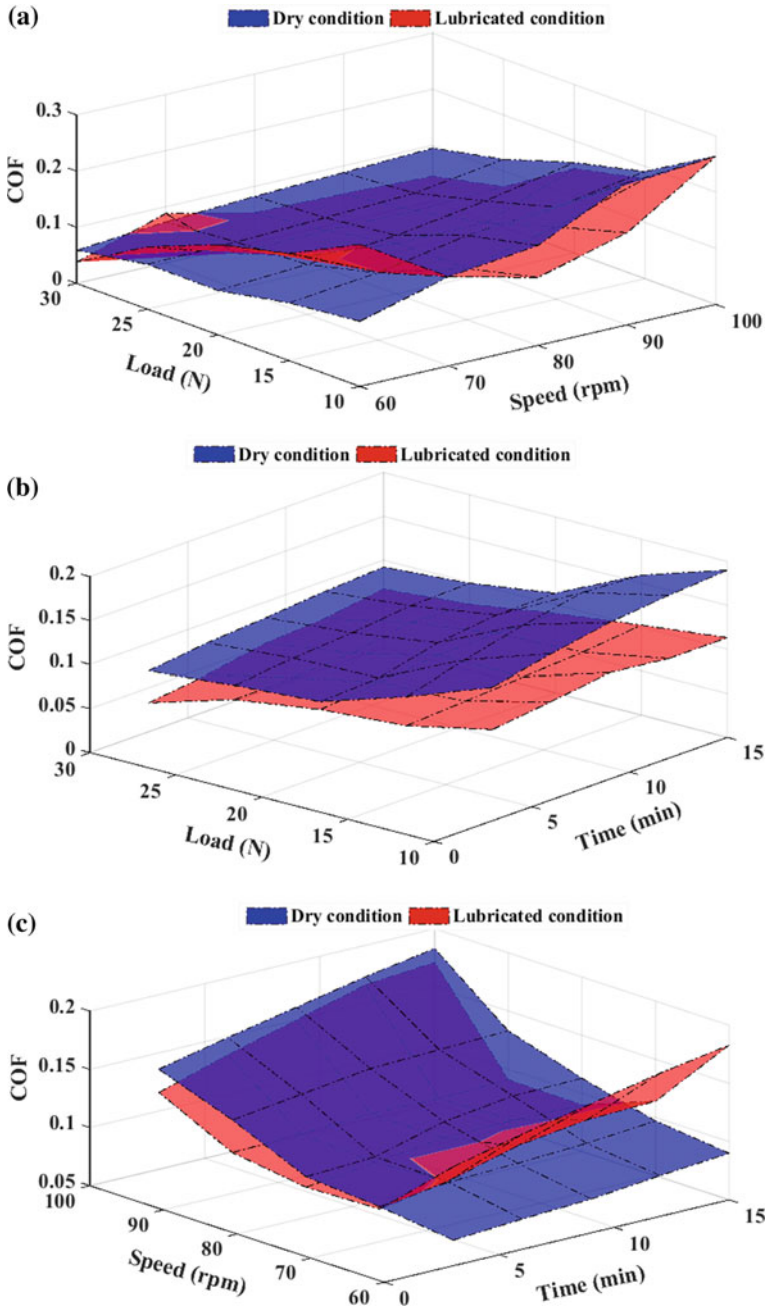
Fig. 3.21 Comparative study of friction behaviour of Ni–B coating under dry and lubricated condition **a** load versus speed, **b** load versus time and **c** speed versus time
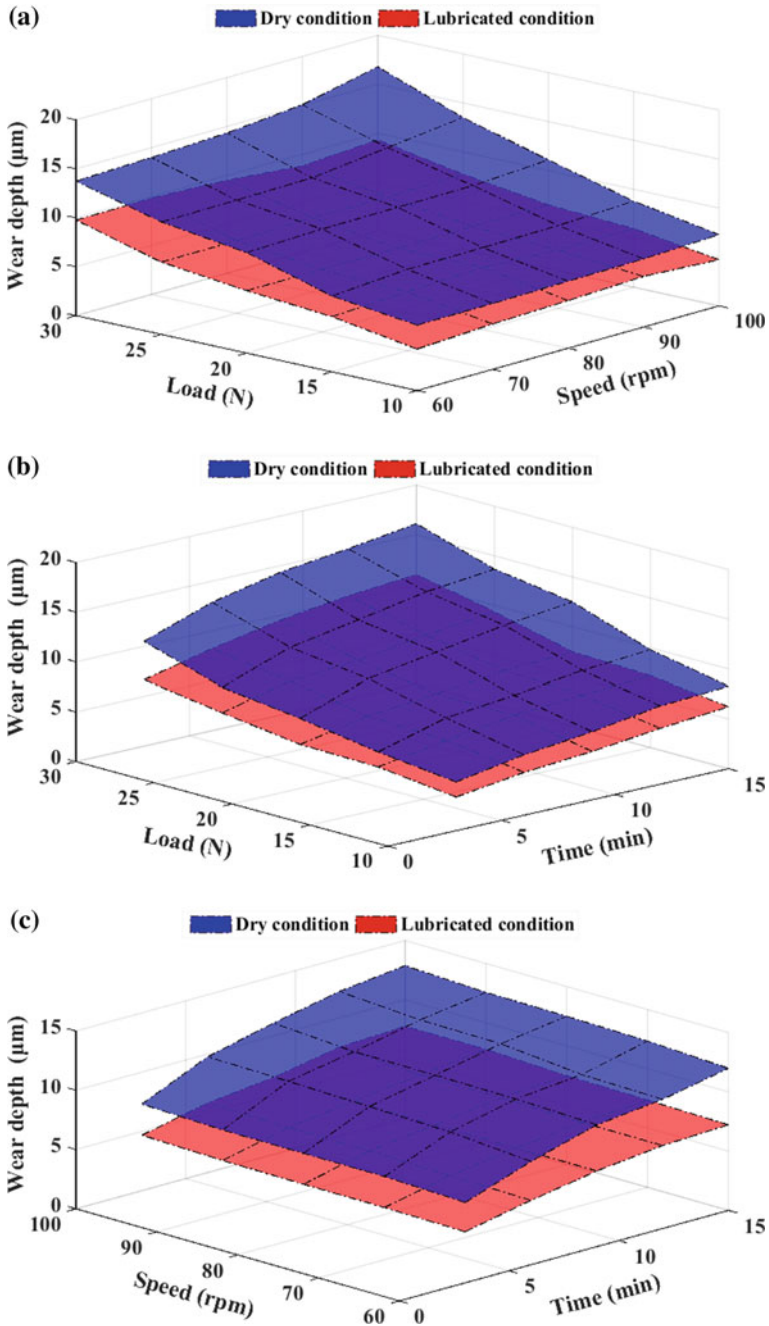
Fig. 3.22 Comparative study of wear behaviour of Ni–B coating under dry and lubricated condition **a** load versus speed, **b** load versus time and **c** speed versus time

variation of wear depth with applied load and sliding duration (Fig. 3.22b) as well as speed and time (Fig. 3.22c) are almost same. In all the three cases, wear depth increases with an increase in values of the tribological test parameters. The variation of wear depth under dry condition is also noticed to be in accordance with Archard's law. Furthermore, the wear depth under lubricated condition is significantly lower compared to dry condition. Therefore, tribological characteristics of the coatings improve under lubrication. This may be attributed to the self-lubricating nature of Ni–B deposits, i.e. the cauliflower-like microstructure, the ability of the columnar growths to retain lubricants and the flowing lubricant carrying away heat as well as wear debris generated along with it.

3.3.2.4 Microstructure Study of the Worn-Out Surfaces

The SEM image of the worn surface of a heat-treated Ni–B coating under dry condition is shown in Fig. 3.23a. The coatings are seen to undergo very less wear. Grooves may be observed along the sliding direction. Coating delamination or adhesion patches are also not visible. This is indicative of mild abrasive wear being the predominant mechanism under dry sliding condition. Resistance to plastic deformation increases due to an increase in hardness [37] preventing adhesion between the coated pins and the counterface disc. Figure 3.23b presents the worn surface of electroless Ni–B coating on which wear tests have been performed under lubricated condition. Fine scratches along sliding direction can be seen. No ploughs or furrows can be seen. Furthermore, the flowing lubricant has a cooling effect, thus reducing the possibility of adhesive wear. The wear mechanism is fundamentally mild abrasive in nature. Since the columnar structure of electroless Ni–B coating helps in retaining lubricant, a very low COF is indicated. A similar phenomenon is confirmed from the SEM micrograph of the worn surface (Fig. 3.23). Blackish patches may be may be seen due to the retained lubricant as well as formation of oxide layers.
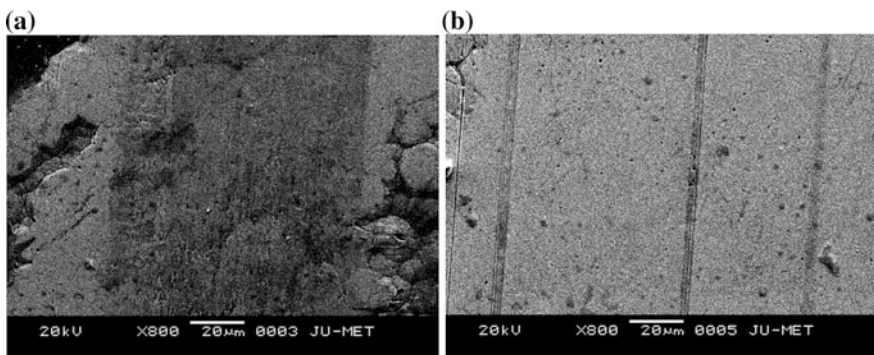

Fig. 3.23 SEM micrograph of wear track of Ni–B coating tested at **a** dry condition and **b** lubricated condition

3.4 Conclusion

In this investigation, electroless Ni–B coating has been deposited on mild steel substrate. Characterization of the deposited Ni–B coating has been done utilizing SEM, EDX and XRD technique. Microhardness and surface roughness are studied utilizing Vickers micro-indentation method and surface profilometry, respectively. Variations of friction and wear are studied under dry and lubricated conditions. Wear mechanism of coatings has been also reported. Following conclusions are drawn from the present work:

- The surface of the coating appears grey in as-deposited condition and heat-treated condition. The structure of the heat-treated coated samples resembles the surface of a cauliflower which makes it self-lubricating in nature.
- EDX affirms the presence of Ni and B in the coating. The B content is almost 7.51% by weight.
- The XRD plots reveal that the deposits are amorphous in as-deposited condition while it becomes crystalline on heat treatment due to the precipitation of nickel borides (Ni_2B and Ni_3B).
- Average values of hardness in as-deposited and heat-treated (1 h at 350 °C) condition are seen to be 855 $HV_{0.5}$ and 1160 $HV_{0.5,}$ respectively.
- R_a of the coatings is found to be ~ 0.7–0.8 μm.
- Investigation of the tribological characteristics of the coatings under dry and lubricated condition indicates that Ni–B is suitable as a tribo-coating under lubricated condition. This is attributed to its inherent self-lubricating capabilities and columnar structures that act as retainer of lubricant.
- The wear mechanism under dry and lubricated condition is seen to be mild abrasive.

From the present study, it may be concluded that electroless Ni–B coatings have good friction and wear reduction capabilities under the influence of a lubricant. The coatings may find use in applications where tribological contact takes place under lubricated condition.

References

1. Mellor, B.G.: Surface Coatings for Protection Against Wear. Woodhead Publishing Series, Cambridge (2006)
2. Wurtz, A.: C. R. Hebd. Seances Acad. Sci. **18**, 702–705 (1844)
3. Brenner, A., Riddell, G.E.: Nickel coating on steel by chemical reduction. J. Res. Natl Bur. Stand. **37**(1), 31–34 (1946)
4. Mallory, G.O., Hadju, J.B.: Electroless Plating: Fundamentals and Applications. AESF, Orlando (1990)
5. Agarwala, R.C., Agarwala, V.: Electroless alloy/composite coatings: a review. Sadhana **28**(3–4), 475–493 (2003)

6. Hur, K.H., Jeong, J.H., Lee, D.N.: Microstructure and crystallization of electroless Ni–P deposits. J. Mater. Sci. **25**(5), 2573–2584 (1990)
7. Sahoo, P.: Wear behaviour of electroless Ni–P coatings and optimization of process parameters using Taguchi method. Mater. Des. **30**(4), 1341–1349 (2009)
8. Anik, M., Körpe, E., Sen, E.: Effect of coating bath composition on the properties of electroless nickel–boron films. Surf. Coat. Technol. **202**(9), 1718–1727 (2008)
9. Das, S.K., Sahoo, P.: Tribological characteristics of electroless Ni–B coating and optimization of coating parameters using Taguchi based grey relational analysis. Mater. Des. **32**, 2228–2238 (2011)
10. Das, S.K., Sahoo, P.: Optimization of electroless Ni-B coatings based on multiple roughness characteristics. J. Tribol. Surf. Eng. **2**(1/2), 85–106 (2011)
11. Mukhopadhyay, A., Duari, S., Barman, T.K., Sahoo, P.: Tribological performance optimization of electroless Ni–B coating under lubricated condition using hybrid grey fuzzy logic. J. Inst. Eng. (India): Ser. D **97**(2), pp. 215–231 (2016)
12. Steinmetz, P., Alperine, S., Friant-costantini, A., Josso, P.: Electroless deposition of pure nickel, palladium and platinum. Surf. Coat. Technol. **43–44**, 500–510 (1990)
13. Riedel, W.: Electroless Nickel Plating. ASM International, Metals Park, OH (1991)
14. Sahoo, P., Das, S.K.: Tribology of electroless nickel coatings–A review. Mater. Des. **32**, 1760–1775 (2011)
15. Lowenheim, F.A.: Electroplating: Fundamentals of Surface Finishing. McGraw- Hill Book Co, New York (1978)
16. Elansezhian, R., Ramamoorthy, B., Nair, P.K.: The influence of SDS and CTAB surfactants on the surface morphology and surface topography of electroless Ni–P deposits. J. Mater. Process. Technol. **209**(1), 233–240 (2009)
17. Allen, R.M., VanderSande, J.B.: The structure of electroless Ni-P films as function of composition. Scripta Metall. **16**(10), 1161–1164 (1982)
18. Berkh, O., Eskin, S., Zahavi, J.: Properties of electrodeposited Ni-P-SiC composite coatings. Met. Finish. **94**(3), 35–40 (1996)
19. Baudrand, D., Bengston, J.: Electroless plating processes: developing technologies for electroless nickel, palladium and gold. Met. Finish. **93**(9), 55–57 (1995)
20. Apachitei, I., Duszczyk, J., Katgerman, L., Overkamp, P.J.B.: Electroless Ni-P composite coatings: the effect of heat treatment on the microhardness of substrate coating. Scripta Mater. **38**(9), 1347–1353 (1998)
21. Apachitei, I., Tichelaar, F.D., Duszczyk, J., Katgerman, L.: The effect of heat treatment on the structure and abrasive wear resistance of autocatalytic NiP and NiP–SiC coatings. Surf. Coat. Technol. **149**(2–3), 263–278 (2002)
22. Vitry, V., Delaunois, F., Dumortier, C.: Mechanical properties and scratch test resistance of nickel–boron coated aluminium alloy after heat treatments. Surf. Coat. Technol. **202**(14), 3316–3324 (2008)
23. Palaniappa, M., Seshadri, S.K.: Friction and wear behavior of electroless Ni–P and Ni–W–P alloy coatings. Wear **265**(5–6), 735–740 (2008)
24. Staia, M.H., Castillo, E.J., Puchi, E.S., Lewis, B., Hintermann, H.E.: Wear performance and mechanism of electroless Ni-P coating. Surf. Coat. Technol. **86–87**, 598–602 (1996)
25. Ramalho, A., Miranda, J.C.: Friction and wear of electroless NiP and NiP + PTFE coatings. Wear **259**(7–12), 828–834 (2005)
26. Sahoo, P., Pal, S.K.: Tribological performance optimization of electroless Ni–P coatings using the Taguchi method and Grey relational analysis. Tribol. Lett. **28**(2), 191–201 (2007)
27. Srinivasan, K.N., Meenakshi, R., Santhi, A., Thangavelu, P.R., John, S.: Studies on development of electroless Ni–B bath for corrosion resistance and wear resistance applications. Surf. Eng. **26**(3), 153–158 (2010)
28. Balaraju, J.N., Anandan, C., Rajam, K.S.: Morphological study of ternary Ni–Cu–P alloys by atomic force microscopy. Appl. Surf. Sci. **250**(1–4), 88–97 (2005)
29. Balaraju, J.N., Anandan, C., Rajam, K.S.: Electroless deposition of ternary Ni–W–P alloys from sulphate and chloride based baths. Surf. Eng. **21**(3), 215–220 (2005)

30. Das, S.K., Sahoo, P.: Wear performance optimization of electroless Ni-B coating using Taguchi design of experiments. Tribol. Ind. **32**(4), 17–27 (2010)
31. Roy, S., Sahoo, P.: Optimization of electroless Ni-P-W coating for minimum friction and wear using grey Taguchi method, Article ID: 608140. J. Coat **2013**, 1–13 (2013)
32. Roy, S., Sahoo, P.: Friction performance optimization of chemically deposited Ni-P-W coating using Taguchi method, Article ID: 136740. ISRN Tribol. **2013**, 1–9 (2013)
33. Fisher, R.A.: Design of Experiments. Oliver & Boyd, Edinburgh (1951)
34. Montgomery, D.C.: Design and Analysis of Experiments. Wiley, New York (2001)
35. Correa, E., Mejía, J.F., Castaño, J.G., Echeverría, F., Gómez, M.A.: Tribological characterization of electroless Ni–B coatings formed on commercial purity Magnesium. J. Tribol. **139** (5), 051302 (2017)
36. Xu, Y., Zheng, X., Hu, X., Yin, Y., Lei, T.: Preparation of the electroless Ni–P and Ni–Cu–P coatings on engine cylinder and their tribological behaviors under bio-oil lubricated conditions. Surf. Coat. Technol. **258**, 790–796 (2014)
37. Krishnaveni, K., Sankara Narayanan, T.S.N., Seshadri, S.K.: Electroless Ni–B coatings: preparation and evaluation of hardness and wear resistance. Surf. Coat. Technol. **190**(1), 115–121 (2005)